

Regulation of glutamate receptor subunit availability by microRNAs

Julie Karr,¹ Vasia Vagin,² Kaiyun Chen,¹ Subhashree Ganesan,¹ Oxana Olenkina,² Vladimir Gvozdev,² and David E. Featherstone¹

¹Biological Sciences, University of Illinois at Chicago, Chicago, IL 60607

²Institute of Molecular Genetics, Moscow 123182, Russia

The efficacy of synaptic transmission depends, to a large extent, on postsynaptic receptor abundance. The molecular mechanisms controlling receptor abundance are poorly understood. We tested whether abundance of postsynaptic glutamate receptors (GluRs) in *Drosophila* neuromuscular junctions is controlled by microRNAs, and provide evidence that it is. We show here that postsynaptic knockdown of *dicer-1*, the endoribonuclease necessary for microRNA synthesis, leads to large increases in postsynaptic GluR subunit messenger RNA and protein. Specifically, we measured increases in

GluRIIA and GluRIIB but not GluRIIC. Further, knockout of *Mir-284*, a microRNA predicted to bind to GluRIIA and GluRIIB but not GluRIIC, increases expression of GluRIIA and GluRIIB but not GluRIIC proportional to the number of predicted binding sites in each transcript. Most of the depressed GluR protein, however, does not appear to be incorporated into functional receptors, and only minor changes in synaptic strength are observed, which suggests that microRNAs primarily regulate *Drosophila* receptor subunit composition rather than overall receptor abundance or synaptic strength.

Introduction

Most synaptic transmission in mammalian brains occurs via glutamate receptors (GluRs). Synthesis and localization of GluRs is essential for brain development, and GluR changes underlie learning, memory, and many different neuropathologies. Several lines of evidence suggest that GluR synthesis may be regulated by microRNAs, which suppress gene expression in a variety of organisms and tissue types (Lee et al., 2007; Baek et al., 2008; Selbach et al., 2008). First, microRNAs are particularly abundant in brains, and have recently been shown to play important roles in several aspects of nervous system development (Cao et al., 2006; Bicker and Schrott, 2008; Fiore et al., 2008). Second, some postsynaptic proteins, possibly including GluR subunits, seem to be locally translated near postsynaptic densities (Sigrist et al., 2000; Job and Eberwine, 2001; Miller et al., 2002; Sutton et al., 2004; Sutton and Schuman, 2005; Martin and Zukin, 2006; Pfeiffer and Huber, 2006; Schuman et al., 2006; Bramham, 2008), whereas the microRNA synthesis protein *dicer* and many microRNAs themselves may be enriched at synapses (Lugli et al., 2005, 2008). Finally, acetylcholine receptor abundance in *Caenorhabditis elegans* neuromuscular

junctions (NMJs) has recently been shown to be regulated by microRNAs (Simon et al., 2008).

Here, we test whether GluR synthesis in *Drosophila melanogaster* is regulated by microRNAs. *Drosophila* NMJs are glutamatergic synapses that are individually identifiable at the cellular level and experimentally accessible throughout development in vivo (Keshishian et al., 1996; Featherstone and Brodie, 2004; Ruiz-Canada and Budnik, 2006). *Drosophila* NMJs contain two biophysically, pharmacologically, and spatially distinct subtypes of ionotropic GluRs (DiAntonio et al., 1999; Marrus et al., 2004; Chen et al., 2005; Featherstone et al., 2005; Qin et al., 2005), called “A type” and “B type.” A-type receptors contain the subunit GluRIIA but not GluRIIB, plus the subunits GluRIIC (also known as GluRIII), GluRIID, and GluRIIE. B-type receptors contain GluRIIB but not GluRIIA, plus GluRIIC, GluRIID, and GluRIIE.

Our results show that microRNAs strongly regulate the abundance of *GluRIIA* and *GluRIIB* GluR subunit mRNAs, and that this has dramatic effects on relative subunit protein abundance. In the absence of microRNA-mediated subunit repression,

Correspondence to David Featherstone: def@uic.edu

Abbreviations used in this paper: AGO1, Argonaute 1; EJC, excitatory junction current; GluR, glutamate receptor; NMJ, neuromuscular junction; sEJC, spontaneous EJC; UTR, untranslated region.

© 2009 Karr et al. This article is distributed under the terms of an Attribution–Noncommercial–Share Alike–No Mirror Sites license for the first six months after the publication date [see <http://www.jcb.org/misc/terms.shtml>]. After six months it is available under a Creative Commons License [Attribution–Noncommercial–Share Alike 3.0 Unported license, as described at <http://creativecommons.org/licenses/by-nc-sa/3.0/>].

GluRIIA and GluRIIB proteins accumulate in the cell; in the absence of a particular microRNA—*MiR-284*—GluR subunits accumulate such that receptor subtype ratios in the synapse are dramatically changed.

Results

Because microRNAs bind to target transcripts via base pairing, a variety of computational methods have been developed that compare the sequence of putative microRNAs with predicted transcripts (Rajewsky, 2006; Watanabe et al., 2007; Bartel, 2009). If appropriate complementarity is detected, an interaction between the microRNA and transcript is presumed to occur in vivo. To determine whether *Drosophila* NMJ GluR transcripts might be regulated by microRNAs and identify candidate microRNAs for each subunit transcript, we bioinformatically screened the entire sequence of *GluRIIA*, *GluRIIB*, *GluRIIC*, *GluRIID*, and *GluRIIE* transcripts for potential microRNA-binding sites. We screened the entire transcript because although it was initially thought that microRNAs selectively associated with untranslated regions (UTRs) to inhibit target translation, microRNAs might also trigger target transcript degradation by binding to complementary sites wherever they might be found in a transcript.

Unfortunately, although we tried several different tools representing several different approaches (Enright et al., 2003; Stark et al., 2003; Brennecke et al., 2005; Krek et al., 2005; Rusinov et al., 2005; Sethupathy et al., 2006), our bioinformatics experiments did not converge toward any usable predictions. To circumvent this problem, we considered a different approach. MicroRNA synthesis requires cleavage of stem-loop precursor RNAs by a protein complex containing the type III ribonuclease “dicer” (Bernstein et al., 2001; Hutvagner et al., 2001). Indeed, the property of being processed by dicer is one of the classical definitions of a microRNA (Berezikov et al., 2006). Therefore, if GluR transcripts are regulated by microRNAs, then they must also be regulated (indirectly) by dicer. Specifically, eliminating dicer function should increase GluR protein abundance if GluR transcripts are regulated by microRNAs. Elimination of dicer should also cause an increase in GluR mRNA abundance if microRNAs regulate GluR transcript stability (as opposed to translation).

The *Drosophila* genome encodes two dicer paralogs: dicer-1 and dicer-2. Dicer-1 and dicer-2 interact with different sets of proteins and have functionally distinct roles in vivo: dicer-1 preferentially cleaves precursor microRNAs after they are exported from the nucleus, whereas dicer-2 preferentially cleaves exogenous double-stranded RNA, presumably as a defense against viral infection (Lee et al., 2004). Elimination of dicer-1 function should therefore prevent synthesis of *Drosophila* microRNAs, allowing us to determine whether NMJ GluRs are regulated by microRNAs. Unfortunately, consistent with the fact that dicer is required for early development in every complex organism examined to date (Giraldez et al., 2005; Murchison et al., 2005), *Drosophila* dicer-1 mutants (*Dcr-1[d102]* and *Dcr-1[1147X]*) died in embryogenesis before proper NMJ formation and GluR expression. We also examined “semiviable”

ago1[04845] mutants. Argonaute 1 (AGO1), like dicer-1, is thought to be preferentially required for microRNA synthesis (Okamura et al., 2004). However, homozygous *ago1[d04845]* mutants, like dicer mutants, also died before normal NMJ formation and GluR expression.

As a result, we were unable to use dicer-1 (or AGO1) mutants to test whether NMJ GluRs are regulated by microRNAs. Such an analysis would have been, in any case, complicated by possible presynaptic microRNA-dependent changes affecting transsynaptic induction of receptor expression (Broadie and Bate, 1993). However, the previously described segregation of dicer-1 and dicer-2 function in *Drosophila* (Lee et al., 2004) suggested another possible approach. If dicer-1 is preferentially required for microRNA synthesis, but dicer-2 is preferentially required for processing of exogenous double-stranded RNA (Lee et al., 2004), then it should be possible to knock down dicer-1 function via RNAi (Fig. 1 A). RNAi knockdown of dicer-1 might be more permissive for development (and thus study of GluR expression) than mutants for two reasons: (1) RNAi typically reduces, but does not eliminate, target function; and (2) RNAi transgene expression in *Drosophila* can be temporally and spatially restricted using the *Gal4-UAS* system (Brand and Perrimon, 1993), allowing us to knock down dicer-1 only in postsynaptic muscle cells while leaving all other tissues as wild type.

To test this approach, we generated a *UAS-dicer-1 RNAi* transgene. Global expression of this transgene using a tubulin *Gal4* driver (*TubGal4/UAS-dcr1.RNAi*; Lee and Luo, 1999) caused early embryonic lethality, similar to that observed in dicer-1 and AGO1 mutants. In contrast, expression of dicer-1 RNAi specifically in postsynaptic body wall muscles (*24BGal4/UAS-dcr1.RNAi*) allowed animals to hatch, feed, and develop through third instar larval stages. To confirm that body wall muscle dicer-1 was knocked down in these animals, and to quantify that knockdown, we examined dicer-1 antibody immunoreactivity in third instar larval body wall tissues (Fig. 1, B and C). In control animals, dicer-1 immunoreactivity was prominent as distinct puncta scattered throughout body wall muscle cells (Fig. 1 B). Presumably, these puncta represent micro ribonucleoprotein complexes, with which dicer proteins are thought to associate. However, we also observed dicer-1 immunoreactivity as a faint “haze” distributed throughout the muscle cells (Fig. 1 B). Body wall muscles expressing dicer-1 RNAi showed a dramatic decrease in both haze intensity and number of dicer-1 immunoreactive puncta, which is consistent with elimination of approximately two thirds of muscle dicer-1 (Fig. 1, B and D).

MicroRNAs can repress gene expression by decreasing target transcript abundance or by suppressing translation. To test whether NMJ GluR transcript abundance is dependent on dicer-1 (and thus regulated by microRNAs), we measured *GluRIIA* and *GluRIIB* transcript abundance (using quantitative real-time RT-PCR and FISH) in control animals and in animals expressing *dicer-1 RNAi* specifically in postsynaptic body wall muscles (*24BGal4/UAS-dcr1.RNAi*). We focused on these two transcripts because GluRIIA and GluRIIB are thought to be rate-limiting for formation of A- and B-type GluRs, respectively;

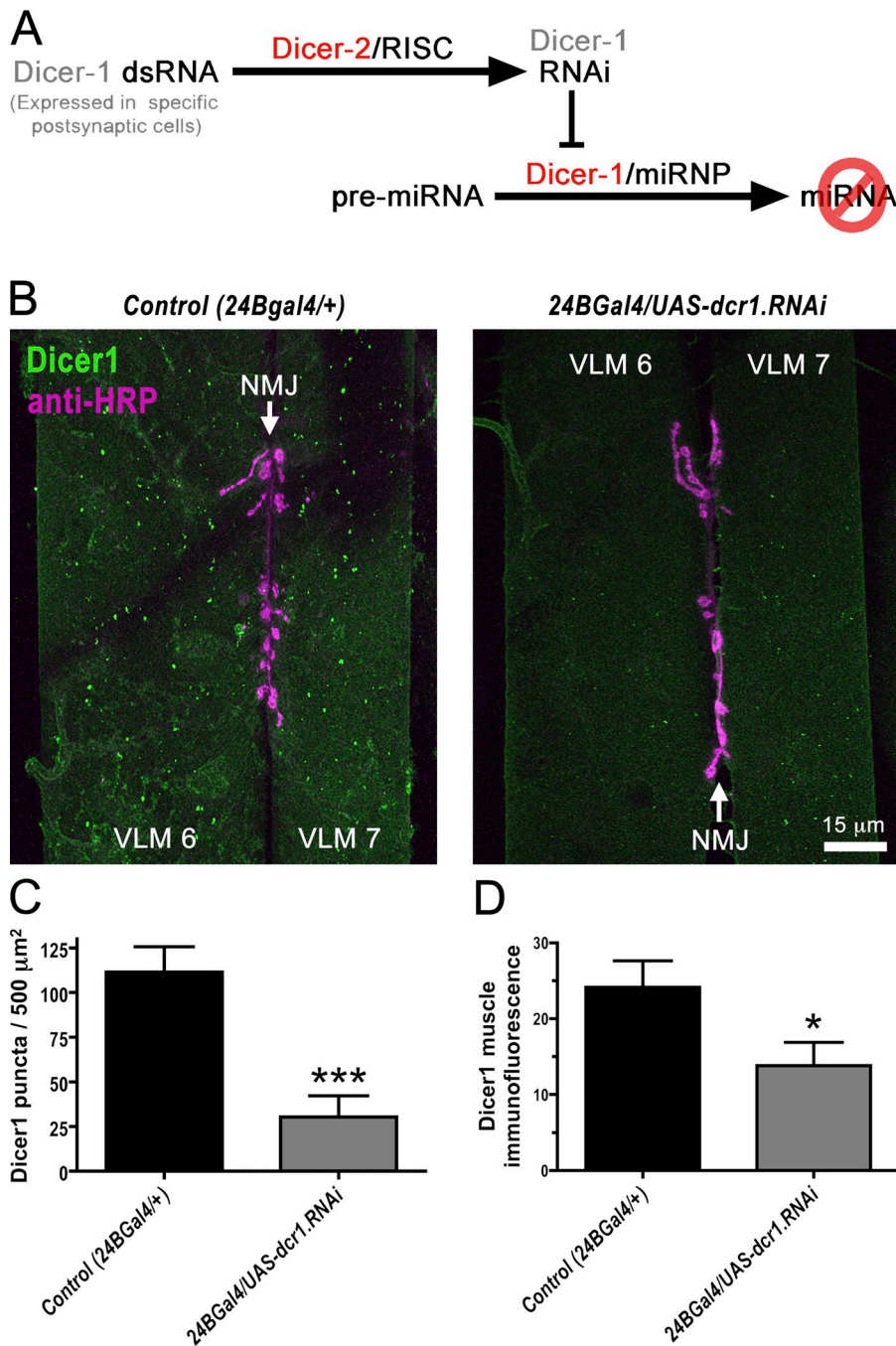


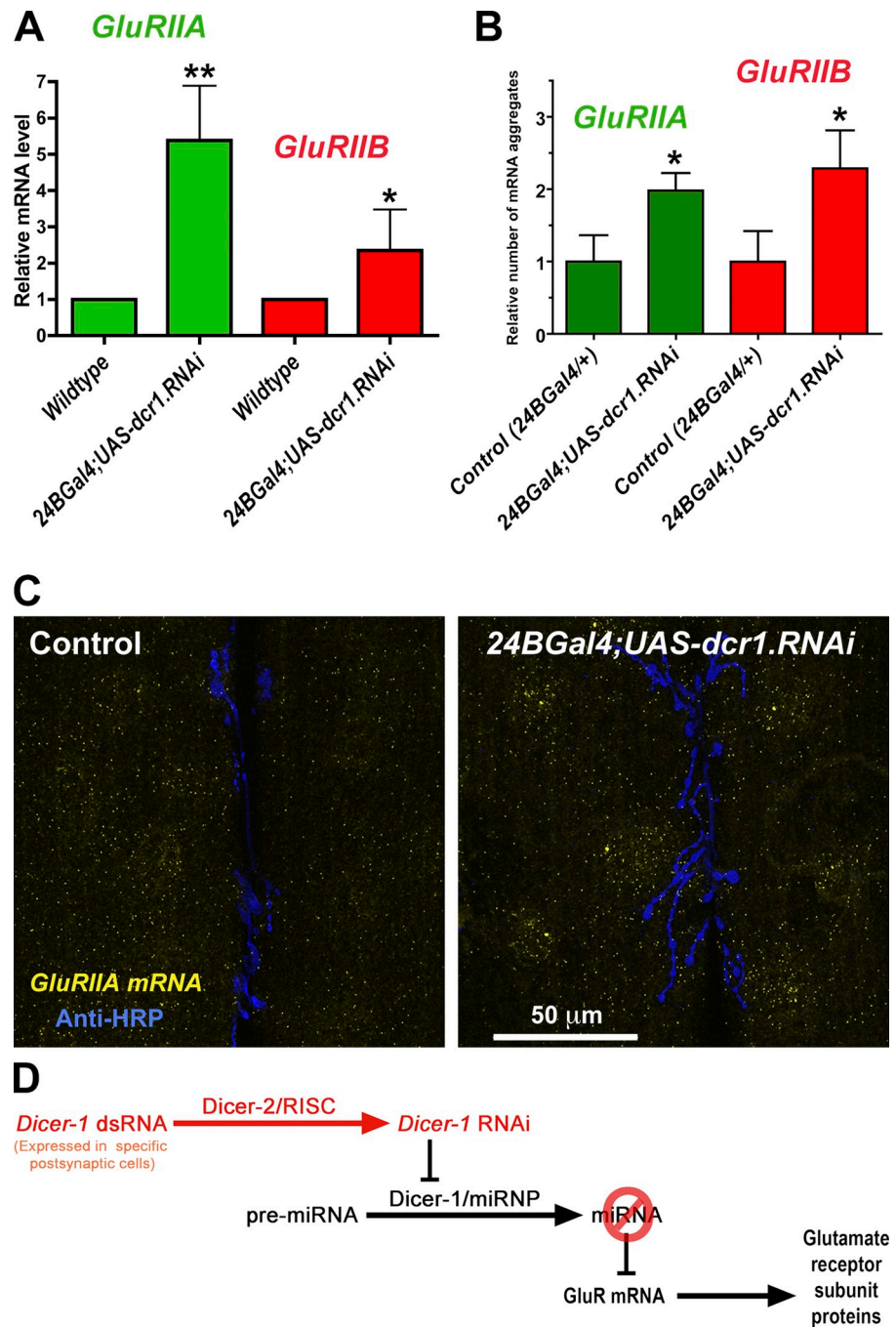
Figure 1. Tissue-specific knockdown of *dicer-1* by tissue-specific expression of *dicer-1* RNAi. (A) Functional segregation of *Drosophila* *dicer-1* (required for microRNA synthesis) and *dicer-2* (required for RNAi) theoretically allows knockdown of *dicer-1* protein by *dicer-1* RNAi. (B) Images show a portion of a single ventral body wall hemisegment in a third instar *Drosophila* larva. Ventral longitudinal muscles 6 and 7 (VLM 6 and VLM 7) are labeled, as are the presynaptic motor terminals (stained with anti-HRP; magenta) that innervate these muscles. In control muscles (24Bgal4/+), *dicer-1* immunoreactivity (green) appears most prominently as puncta scattered throughout the muscle, but also as a faint cytoplasmic haze. In animals expressing *dicer-1* RNAi in muscle cells [24BGal4/UAS-*dcr1*.RNAi], the intensity of the *dicer-1* immunoreactive haze and the number of *dicer-1* puncta are significantly reduced, which is consistent with a large reduction in *dicer-1* in these cells. The differences in *dicer-1* immunoreactive puncta density and overall immunofluorescence are quantified and statistically compared in C and D ($n = 6-7$ for each genotype). Error bars represent SEM. *, $P < 0.01$; ***, $P < 0.0001$.

and *GluRIIA* and *GluRIIB* are expressed only in body wall muscle (DiAntonio et al., 1999). Muscle-specific knockdown of *dicer-1* resulted in large statistically significant increases in *GluRIIA* and *GluRIIB* transcript abundance, as measured by real-time RT-PCR, which is consistent with the idea that stability of both transcripts is regulated by microRNAs (Fig. 2 A). To confirm these results, we used FISH to visualize *GluRIIA* and *GluRIIB* mRNA in body wall muscles of control larvae and larvae expressing *dicer-1* RNAi (Fig. 2 C). Consistent with our real-time RT-PCR results, FISH showed a large increase in *GluRIIA* and *GluRIIB* mRNA abundance after muscle-specific expression of *dicer-1* RNAi (Fig. 2 B). We conclude, based on these results, that *GluRIIA* and *GluRIIB* transcripts are targets

for microRNA-mediated repression, and that the microRNAs that repress *GluRIIA* and *GluRIIB* do so, at least in part, by reducing target transcript abundance. Presumably, this also affects *GluRIIA* and *GluRIIB* protein abundance (Fig. 2 D).

To test whether microRNAs regulate *GluRIIA* and *GluRIIB* protein abundance, we stained larval NMJs using antibodies against *GluRIIA* and *GluRIIB* (Fig. 3). In control animals, most *GluRIIA* and *GluRIIB* protein is tightly localized at synapses, which is consistent with the role of A- and B-type receptors in NMJ transmission. In contrast, very little *GluRIIA* and *GluRIIB* immunoreactivity is detectable in wild-type non-synaptic muscle cell regions. This small amount of immunoreactivity is consistent with a low density of functional nonsynaptic

Figure 2. **Dicer-1 knockdown leads to an increase in GluR mRNA.** (A) Real-time RT-PCR shows that *GluRIIA* and *GluRIIB* mRNA is increased after expression of dicer-1 RNAi in postsynaptic muscles (*24BGal4/UAS-dcr1.RNAi*), compared with wild-type controls ($n = 9-10$ of each genotype). (B) FISH shows a similar increase in *GluRIIA* mRNA in postsynaptic muscles, as measured by density of visible *GluRIIA* mRNA aggregates ($n = 6$ of each genotype). Error bars represent SEM. *, $P < 0.01$; **, $P < 0.001$. (C) Representative FISH images of NMJs on muscles 6 and 7 (as in Fig. 1 B) from control animals and after postsynaptic expression of dicer-1 (*24BGal4/UAS-dcr1.RNAi*). (D) Model explaining how expression of dicer-1 RNAi in body wall muscles could lead to an increase in GluR protein, assuming microRNAs regulate GluR subunit mRNAs.



GluRs measured in previous studies (Nishikawa and Kidokoro, 1995; Featherstone et al., 2000). In *24BGal4/UAS-dcr1.RNAi* larvae, the density of GluRIIA and GluRIIB immunoreactivity at synapses was not different from controls, which was consistent with our electrophysiological results. However, we observed dramatically high levels of nonsynaptic GluRIIA and GluRIIB immunoreactivity in *24BGal4/UAS-dcr1.RNAi* larvae (Fig. 3). Most of this nonsynaptic immunoreactivity was punctate, similar in size and shape to that of synaptic GluR clusters.

To test whether the nonsynaptic GluRIIA and GluRIIB protein puncta observed after expression of *dicer-1* RNAi represented (possibly functional) surface receptors, we used immunocytochemistry and confocal microscopy (Fig. 4). Manually

dissected *24BGal4/UAS-dcr1.RNAi* larvae were briefly incubated with the fixable nonpermeant membrane dye FM1-43FX, in order to label plasma membranes. These preparations were then fixed and stained with GluRIIA and GluRIIB antibodies to label GluRIIA and GluRIIB protein. To determine the spatial relationship of receptor subunit proteins and the muscle plasma membranes, we imaged labeled preparations by confocal microscopy and generated 3D reconstructions of the neuromusculature (Fig. 4). As expected, we observed a high concentration of GluRIIA and GluRIIB immunoreactivity at NMJs (Fig. 4 A, arrows), which likely represents functional synaptic A- and B-type GluRs. There was also a relatively low density of GluRIIA and GluRIIB associated with extrasynaptic plasma membrane,

GluRIIA | GluRIIB | anti-HRP

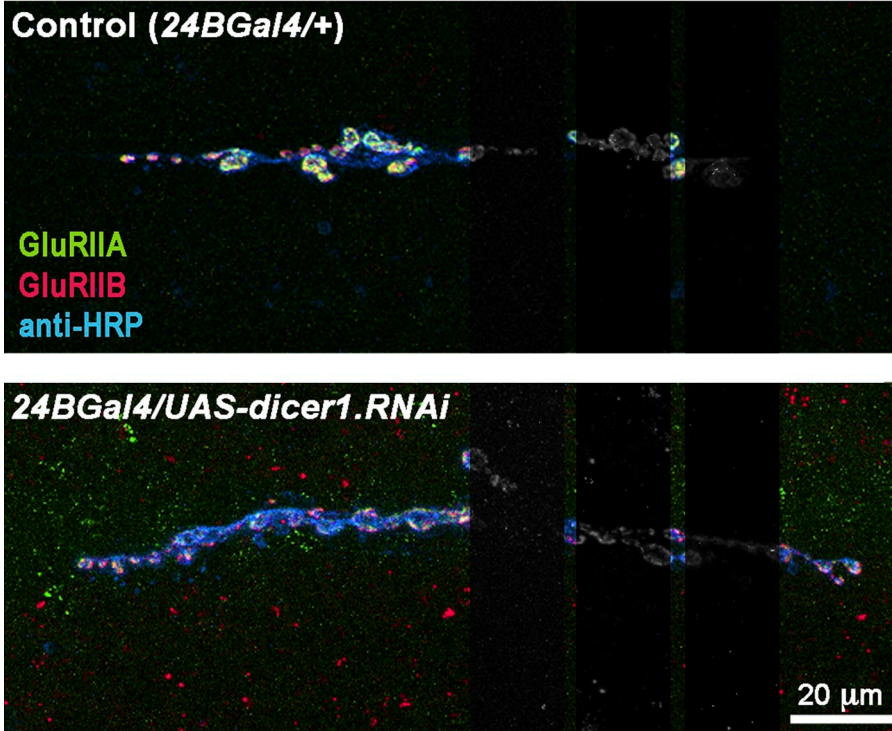
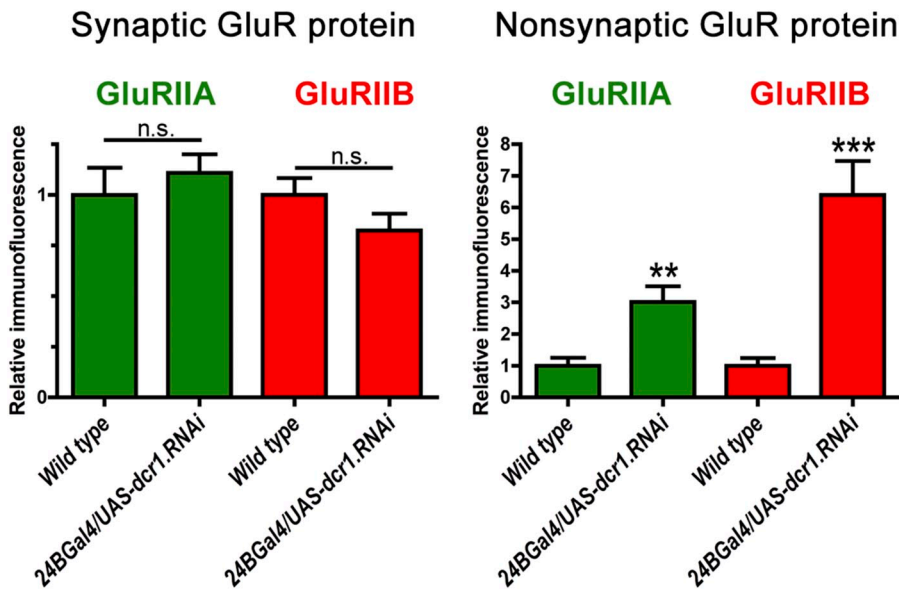


Figure 3. Knockdown of *dicer-1* leads to accumulation of nonsynaptic GluRIIA and GluRIIB protein. The top panels show representative confocal micrographs generated from image stacks of ventral longitudinal muscle 6/7 NMJs stained using antibodies against GluRIIA (green), GluRIIB (red), and HRP (blue). In control NMJs, GluRIIA and GluRIIB protein is incorporated into multimeric GluRs that are localized almost exclusively at NMJs (marked with anti-HRP; blue). When *dicer-1* RNAi is expressed in postsynaptic muscle cells (*24BGal4/UAS-dicer1.RNAi*), the muscle cells show abundant nonsynaptic GluRIIA and GluRIIB immunoreactivity. Three vertical bands pass through the micrographs. These bands each show only fluorescence in one channel: green (GluRIIA), red (GluRIIB), or blue (anti-HRP; left to right, respectively), as grayscale images. Synaptic and nonsynaptic GluR immunoreactivity is quantified on the bottom. The amount of synaptic GluRIIA and GluRIIB is not significantly changed by muscle knockdown of *dicer-1*, but the amount of nonsynaptic GluRIIA and GluRIIB is increased 300–600% ($n = 12$ for each genotype). Error bars represent SEM. n.s., not significant. **, $P < 0.001$; ***, $P < 0.0001$.



which is consistent with the presence of some functional extrasynaptic receptors. However, the vast majority of GluRIIA and GluRIIB immunoreactivity in *24BGal4/UAS-dcr1.RNAi* larval muscles was distributed inside the thin layer of FM1-43 fluorescence representing the muscle plasma membrane (Fig. 4, A, B, D, and E), which suggests that the ectopic GluRIIA and GluRIIB protein observed in this genotype is mainly in the interior of muscle cells. We conclude, based on this evidence, that although *dicer-1* knockdown dramatically increases abundance of GluRIIA and GluRIIB protein, most of the de-repressed excess GluRIIA and GluRIIB is nonfunctional and distributed throughout the interior of the muscle cells.

Intracellular GluRIIA and GluRIIB could represent assembled GluRs unable to traffic to plasma membranes, or they could represent subunit protein that is not assembled into a receptor complex. The former suggests that GluRs are assembled early and then distributed throughout postsynaptic cells, whereas the latter suggests that unassembled GluR protein might be widely distributed before being assembled into multimeric receptors. To determine whether extrasynaptic intracellular GluRIIA and GluRIIB immunoreactivity might represent assembled but intracellular GluRs, we examined immunoreactivity for the essential receptor subunit GluRIIC (also known as GluRIII; Marrus et al., 2004). GluRIIC is a required subunit in

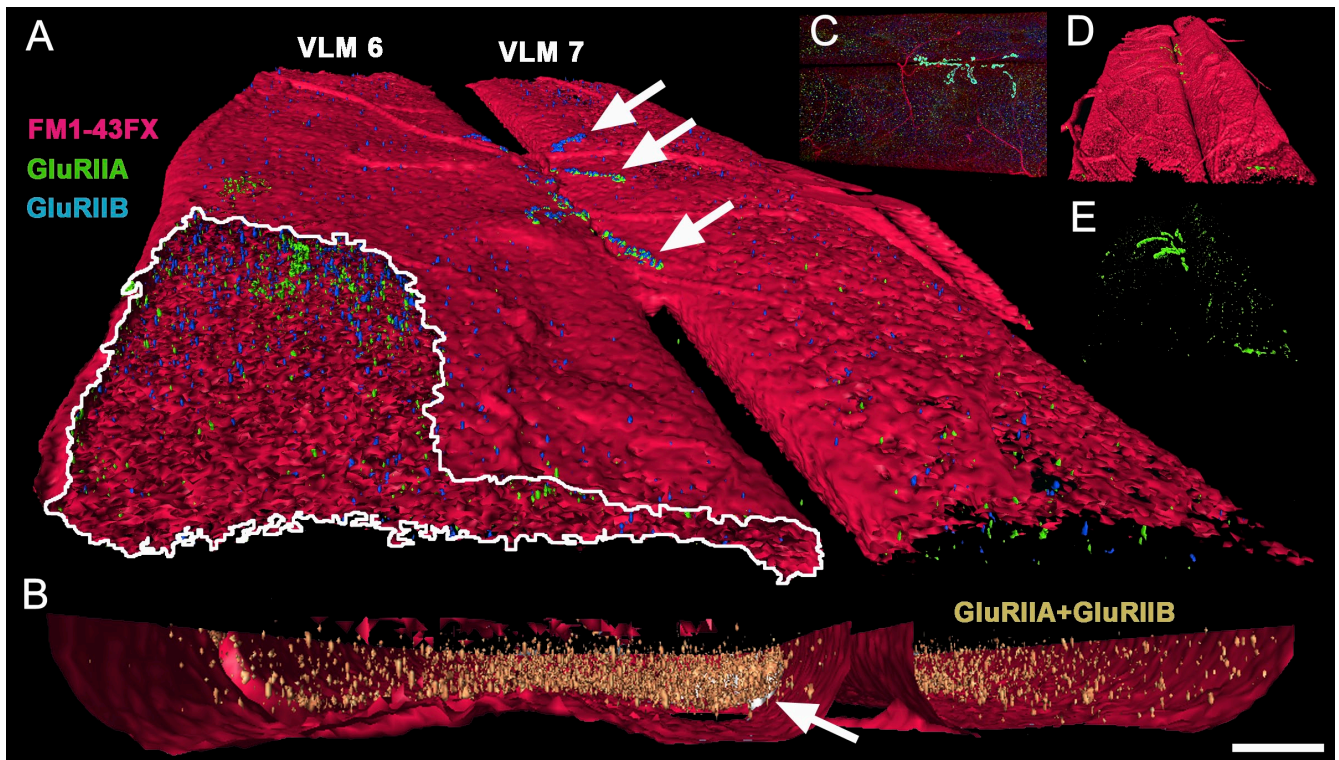


Figure 4. **Nonsynaptic GluRIIA and GluRIIB protein is intracellular.** (A) 3D confocal reconstruction of ventral longitudinal muscle (VLM) 6 and 7 from a *24BGal4/UAS-dicer-1.RNAi* larvae. Before fixation, the muscle plasma membranes were stained by FM1-43FX (red). In the NMJ (arrows), GluRIIA (green) and GluRIIB (blue) immunoreactivity is visibly associated with the plasma membrane. However, as shown by the “cut-away” plasma membrane section of VLM 6 (bottom left), most of the GluRIIA and GluRIIB immunoreactivity is intracellular and obscured by the membrane staining. (B) 3D reconstruction of the ventral portion of another VLM 6 and 7, viewed in cross section to show abundant intracellular GluRIIA and GluRIIB protein (gold). Bar, 10 μ m. (C) Confocal stack of the images used to create the image in A. (D) 3D reconstruction, as in A, showing only muscle plasma membrane (red) and GluRIIA (green). Note the GluRIIA protein associated with the NMJ. (E) Same data shown in D, but with the red muscle membrane not shown. Note the abundant GluRIIA that was previously obscured by the plasma membrane, which is consistent with the nonsynaptic GluRIIA being intracellular.

both A- and B-type GluRs (Marrus et al., 2004). Therefore, if GluRIIC immunoreactivity in *24BGal4/UAS-dicer-1.RNAi* larvae is not associated with nonsynaptic GluRIIA or GluRIIB immunoreactivity, then the GluRIIA and GluRIIB immunoreactivity cannot represent assembled receptors. As shown in Fig. 5, GluRIIC immunoreactivity in *24BGal4/UAS-dicer-1.RNAi* larvae matched that observed in controls. We therefore conclude that the abundant nonsynaptic intracellular GluRIIA and GluRIIB protein observed in *24BGal4/UAS-dicer-1.RNAi* larvae (Figs. 3 and 4) represents GluR subunits unable to multimerize, perhaps because of the relatively restricted availability of other required subunits.

To confirm our immunocytochemical results, we turned to voltage-clamp electrophysiology (Fig. 6). Electrophysiology is extremely sensitive to changes in functional GluR abundance and distribution; in the *Drosophila* larval NMJ, differences of only a few dozen individual postsynaptic receptors can be reliably detected and statistically differentiated using this method. First, we measured total synaptic strength by stimulating the presynaptic motor nerve and measuring the amplitude of the resulting postsynaptic excitatory junction currents (EJCs). EJCs in *24BGal4/UAS-dicer-1.RNAi* larvae were slightly, but not significantly, larger than those in controls (Fig. 6 A). The frequency of spontaneous EJCs (sEJCs) was not significantly altered in *24BGal4/UAS-dicer-1.RNAi* larvae compared with controls (Fig. 6 B).

However, *24BGal4/UAS-dicer-1.RNAi* larvae showed a small but significant increase in sEJC amplitude, which suggests a slight increase in the number of postsynaptic GluRs (Fig. 6, C and D). To specifically check for changes in the number of functional nonsynaptic receptors, we pressure-ejected 1 mM glutamate onto extrasynaptic muscle membrane in control and *24BGal4/UAS-dicer-1.RNAi* larvae. The amplitude of nonsynaptic GluR currents was not increased in *24BGal4/UAS-dicer-1.RNAi* larvae, compared with controls (Fig. 7). We conclude, based on our electrophysiology, that *dicer-1* knockdown has very little effect on total numbers of functional postsynaptic GluRs, and no effect on the number of functional nonsynaptic receptors. These results are consistent with our immunocytochemical results (Figs. 2–5).

The data described above suggest that: (1) *Drosophila* GluRs are indeed regulated by microRNAs; (2) this regulation occurs, at least in part, via degradation of *GluRIIA* and *GluRIIB* subunit transcripts; and (3) microRNA-mediated regulation of GluRIIA and GluRIIB may be most important for control of receptor assembly and/or subunit composition rather than synaptic strength. However, these data do not address the possibility that regulation of GluRIIA and GluRIIB occurs indirectly (via regulation of an unknown transcript that in turn regulates GluR transcript abundance and/or receptor assembly). Nor do the data reconcile the apparent discrepancy between bioinformatic predictions and the

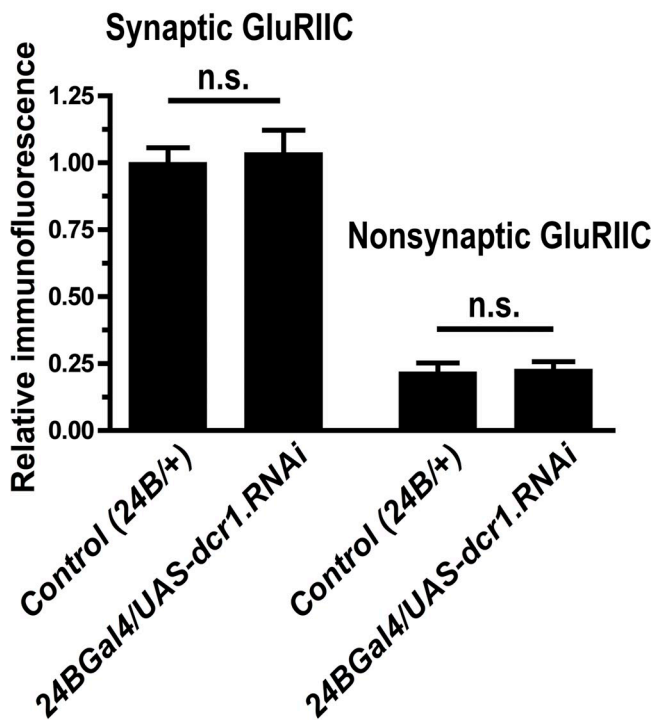
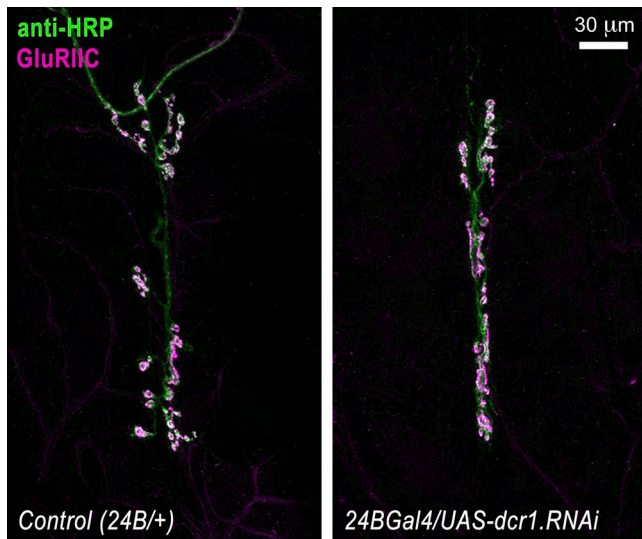


Figure 5. Knockdown of *dicer-1* does not alter abundance or distribution of GluRIIC protein. GluRIIC protein distribution is normal after muscle-specific knockdown of *dicer-1*; all GluRIIC remains tightly localized to NMJs in both control and 24BGal4/UAS-*dicer-1*.RNAi larvae. (bottom) Quantification from preparations like those shown in the micrographs ($n = 10\text{--}15$ for each genotype). Error bars represent SEM. n.s., not significant.

phenotypes observed in 24BGal4/UAS-*dcr1*.RNAi larvae. To address these problems, we returned to bioinformatics.

The lack of the GluRIIC phenotype in 24BGal4/UAS-*dcr1*.RNAi larvae indicated that *GluRIIC* transcripts are not regulated by microRNAs in vivo. Given this, we reasoned that it might be possible to fine-tune bioinformatic search parameters such that the algorithm could simultaneously predict microRNA-binding sites in *GluRIIA* and *GluRIIB*, which is consistent with our experimental results, but no (or relatively few) microRNA-binding sites in *GluRIIC*, which is also consistent with our experimental

results. Many published algorithms predict no microRNA-binding sites in *GluRIIA*, *GluRIIB*, or *GluRIIC* transcripts, which suggests that these algorithms are too restrictive. Several of these algorithms assume highly complementary microRNA–target binding, which has subsequently been shown to not be absolutely required for microRNA-mediated transcript inhibition (Rajewsky, 2006). In contrast, the “MicroInspector” algorithm of Rusinov et al. (2005) is designed to identify all possible sites of microRNA–target interaction, which can then be sorted according to predicted strength. Using default/recommended parameters (25°C hybridization, -26 kcal/mol free energy cutoff), MicroInspector (version 1.0) predicted 106 binding sites for 43 different *Drosophila* microRNAs in the *GluRIIA* transcript, 91 binding sites for 43 different microRNAs in the *GluRIIB* transcript, and 132 binding sites for 45 different microRNAs in the *GluRIIC* transcript (see Tables S1–S3). The predicted binding sites in each case were scattered throughout the entire transcript (Tables S1–S3).

To restrict the parameters such that MicroInspector’s predictions were more consistent with our experimental results, we sorted the entire set of predicted interactions according to the calculated free energy of binding, and selected parameters that would predict microRNA-binding sites in *GluRIIA* and *GluRIIB* but not *GluRIIC*. Specifically, we found that 20°C hybridization and a more restrictive free energy cutoff of -37.1 kcal/mol predicted two binding sites (for *MiR-284* and *MiR-306*) in *GluRIIA*, two binding sites (both for *MiR-284*) in *GluRIIB*, and zero binding sites in *GluRIIC* (Fig. 8 A). Interestingly, none of the predicted binding sites in *GluRIIA* or *GluRIIB* were in UTRs. However, there is no a priori reason to assume that microRNA-binding sites must be in UTRs, as the *dicer*-dependent loss of *GluRIIA* and *GluRIIB* transcript that we observed could theoretically be triggered by microRNA binding to any region of the transcript, including protein-coding sequences.

If *MiR-284* regulates *GluRIIA* and *GluRIIB*, then *MiR-284* loss-of-function mutants should show large increases in *GluRIIA* and *GluRIIB* similar to or (more likely) larger than those observed after *dicer-1* knockdown. To test this, we examined *GluRIIA* and *GluRIIB* protein distribution in homozygous *Df(3R)kar-Sz12* mutant larvae, in which the *MiR-284* gene is deleted. Homozygous *Df(3R)kar-Sz12* mutants were 100% prepupal lethal, but a small fraction (<1%) of animals survived to the third instar larval stage. The behavior and gross morphology of *Df(3R)kar-Sz12* animals appeared normal by light microscopy, except for a tendency toward slightly swollen bodies and increased “bursting” when cuticles were initially penetrated for dissection, which suggests increased hemolymph pressure or weaker body walls. Importantly, light microscopic examination of dissected *Df(3R)kar-Sz12* larvae showed relatively normal neuromuscular anatomy.

As shown in Fig. 8 B, homozygous *Df(3R)kar-Sz12* mutant larvae showed dramatic increases in nonsynaptic *GluRIIA* and *GluRIIB* protein, which is consistent with the revised bioinformatic predictions (Fig. 8 A). Specifically, nonsynaptic *GluRIIA* was increased $\sim 500\%$, and nonsynaptic *GluRIIB* was increased $\sim 2,800\%$ (Fig. 8 C). As with knockdown of *dicer-1* by RNAi, synaptic *GluRIIA* was not increased in *Df(3R)kar-Sz12* larvae.

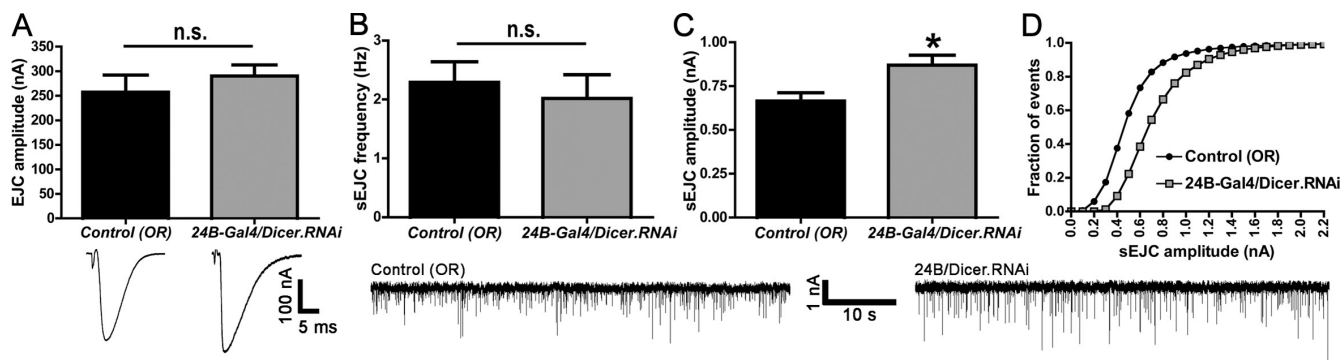


Figure 6. **NMJ synaptic transmission is largely unaltered after muscle-specific knockdown of dicer-1 RNAi.** Synaptic transmission was assayed by voltage-clamping postsynaptic ventral longitudinal muscle 6 (at -60 mV) and recording either evoked (EJC) or spontaneous (sEJC) synaptic transmission at NMJs. (A) EJC amplitude is not significantly changed after muscle-specific knockdown of dicer-1 ($n = 8-10$ for each genotype). (B) Knockdown of muscle dicer-1 also does not significantly change sEJC ("mini") frequency ($n = 10-20$ animals of each genotype; thousands of sEJCs). (C and D) Muscle-specific knockdown of dicer-1 leads to a slight increase in sEJC amplitude, which suggests a slight increase in the number of functional postsynaptic GluRs ($n = 10-20$ animals of each genotype; thousands of sEJCs). Error bars represent SEM. n.s., not significant. *, $P < 0.01$.

Synaptic GluRIIB immunoreactivity, however, was increased $\sim 250\%$ in *Df(3R)kar-Sz12* larvae (Fig. 8 C). In contrast to GluRIIA and GluRIIB, the abundance and distribution of GluRIIC immunoreactivity in *Df(3R)kar-Sz12* larvae matched that of wild-type controls (Fig. 8 D), which is consistent with the conclusion that *GluRIIC* mRNA is not regulated by *MiR-284*. Interestingly, microRNA-mediated repression of *GluRIIA* and *GluRIIB* seemed to be dose dependent, in that *GluRIIB*, with two predicted *MiR-284* binding sites, was much more strongly de-repressed after knockout of *MiR-284* than was *GluRIIA*, which has only one predicted *MiR-284* binding site.

To confirm that the *Df(3R)kar-Sz12* mutant phenotype shown in Fig. 8 was specifically caused by loss of *MiR-284*, we performed two types of experiments. First, we performed a complementation test using another *MiR-284* deletion, *Df(3R)exel7317*. As expected, *Df(3R)kar-Sz12/Df(3R)exel7317* larvae showed dramatically increased nonsynaptic *GluRIIA* and *GluRIIB* immunoreactivity (Fig. 9 A, left), similar to that observed in homozygous *Df(3R)kar-Sz12* mutants (Fig. 8) and after *dicer-1* knockdown (Fig. 3). Second, we cloned a small genomic fragment containing only the *MiR-284* gene, and expressed this transgene in homozygous *Df(3R)kar-Sz12* mutant larvae, as well as in *Df(3R)kar-Sz12/Df(3R)exel7317* mutant larvae (Fig. 9, A-C).

As shown in Fig. 9 (A-C), transgenic expression of *MiR-284* in both types of *MiR-284* deletion mutant backgrounds rescued *GluRIIA* and *GluRIIB* overexpression phenotypes to near control levels. Expression of the *MiR-284* transgene also rescued both homozygous *Df(3R)kar-Sz12* mutants and *Df(3R)kar-Sz12/Df(3R)exel7317* mutants to adulthood, which suggests that loss of *MiR-284* was by itself responsible for a significant portion of the lethality in these genotypes. Both homozygous *Df(3R)kar-Sz12* mutants and *Df(3R)kar-Sz12/Df(3R)exel7317* mutants showed 100% preadult lethality in the absence of the *MiR-284* transgene.

Significantly, the relatively large increase in GluRIIB abundance relative to GluRIIA abundance that we observed in synaptic receptors after loss of *MiR-284* (Figs. 8 C and 9 B) was also completely rescued, which suggests that *MiR-284* controls postsynaptic GluR subtype ratios. To evaluate this, we computed postsynaptic GluR subtype ratios from unnormalized immunocytochemical data and used them to create pie charts representing relative proportions of A-type (green) and B-type (red) receptors at the NMJ. As shown (Fig. 9 D), wild-type NMJs are slightly enriched for A-type receptors. But after *MiR-284* deletion (mean of *Df(3R)kar-Sz12* and *Df(3R)kar-Sz12/Df(3R)exel7317* phenotypes), the NMJ becomes enriched for

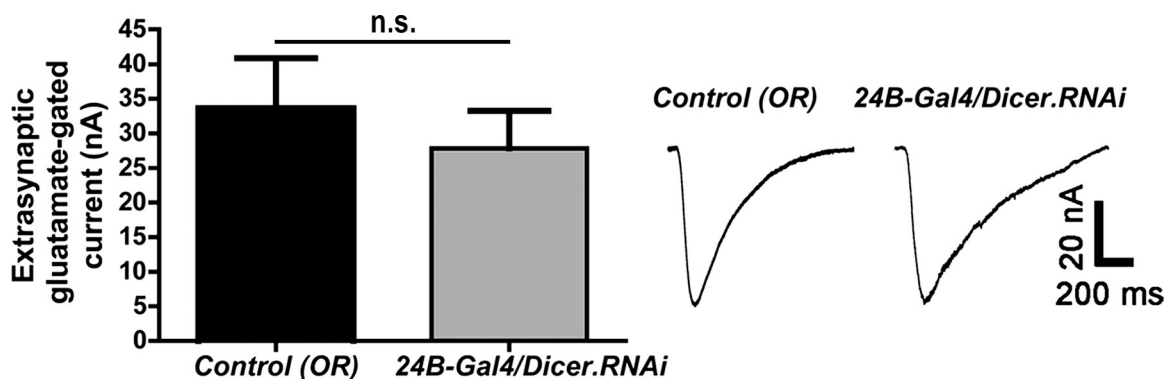


Figure 7. **Knockdown of muscle dicer does not increase the number of functional nonsynaptic GluRs.** Glutamate-gated currents from pressure ejection of 1 mM glutamate onto extrasynaptic muscle plasma membrane are not changed after muscle-specific knockdown of dicer-1 ($n = 11-19$ of each genotype). Error bars represent SEM. n.s., not significant.

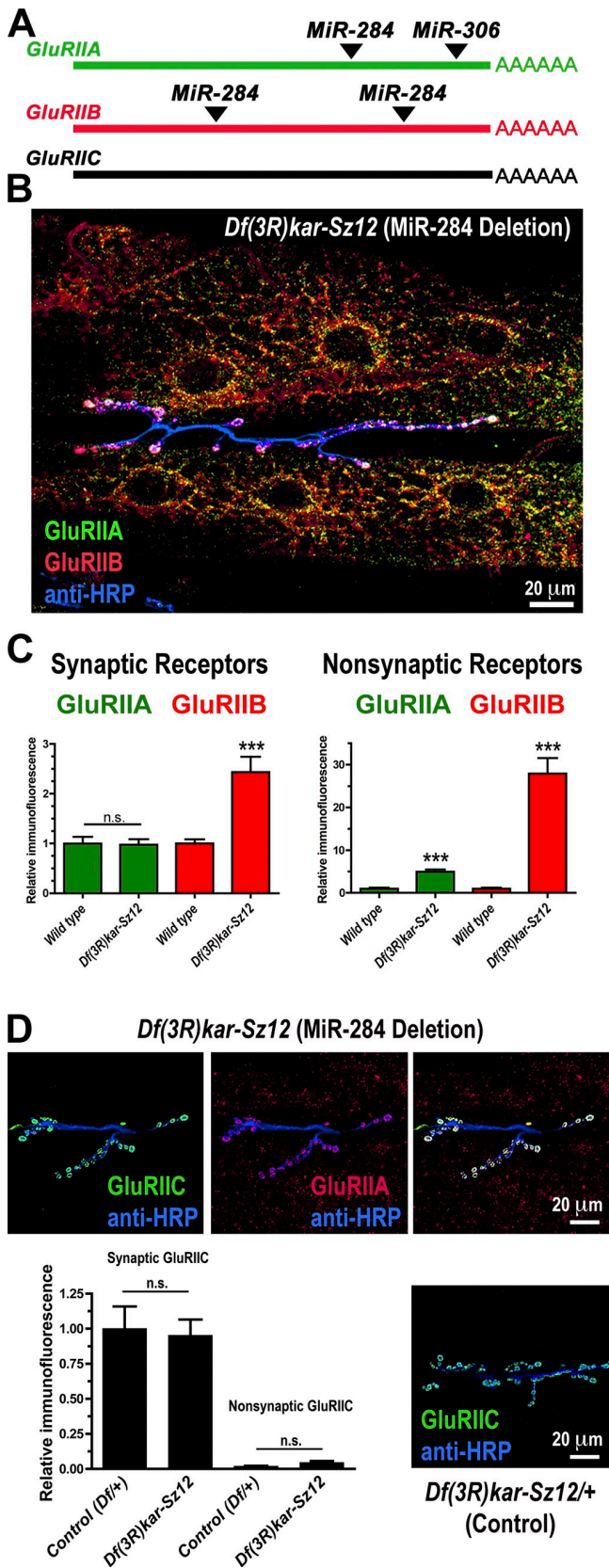


Figure 8. Genetic deletion of *MiR-284* changes synaptic GluR subunit composition and leads to accumulation of nonsynaptic GluRIIA and GluRIIB protein. (A) Type and general location of microRNA-binding sites in *GluRIIA*, *GluRIIB*, and *GluRIIC* mRNAs, based on refined bioinformatics predictions (See main text and Tables S1–S3). (B) Larvae homozygous for

B-type receptors (Fig. 9 D). After transgenic expression of *MiR-284*, this shift in receptor subtype ratio is completely rescued (Fig. 9 D).

Discussion

Our data demonstrate that microRNAs, including but not limited to *MiR-284*, control GluR subunit abundance and synaptic receptor subtype ratios in the *Drosophila* larval NMJ. Specifically, we describe regulation of GluRIIA and GluRIIB. Our conclusion that microRNAs suppress GluRIIA and GluRIIB abundance is based on several pieces of evidence: (1) quantitative real-time PCR showing an increase in *GluRIIA* and *GluRIIB* transcript abundance after *dicer-1* knockdown; (2) FISH showing an increase in microscopically visible *GluRIIA* and *GluRIIB* mRNA after *dicer-1* knockdown; (3) immunohistochemistry showing a dramatic increase in GluRIIA and GluRIIB protein after *dicer-1* knockdown; (4) electrophysiology showing an increase in sEJC amplitude after *dicer-1* knockdown; and (5) immunohistochemistry showing an increase in GluRIIA and GluRIIB protein after genetic deletion of *MiR-284*. To our knowledge, this is the first evidence for regulation of GluRs by small noncoding RNAs in any organism.

Because GluRIIA and GluRIIB are rate-limiting for GluR formation, and because *MiR-284* regulated GluRIIB more strongly compared with GluRIIA, changes in *MiR-284* activity lead to changes in the postsynaptic A-type/B-type receptor ratio. A- and B-type GluRs are biophysically and pharmacologically distinct (DiAntonio et al., 1999; Marrus et al., 2004; Schmid et al., 2008), and the A-type/B-type receptor ratio varies developmentally (Schmid et al., 2008) and along the larval ventral–dorsal axis (Lee et al., 2008). MicroRNA-mediated regulation of GluR subunit transcripts, and *MiR-284* in particular, may explain how these developmental and spatial differences are achieved.

We also showed that RNAi can effectively knock down *Drosophila* *dicer-1*, which is in agreement with the conclusion that *dicer-1* and *dicer-2* play largely independent roles for processing and/or synthesis of microRNA and RNAi (Lee et al., 2004), and demonstrated that *dicer-1* is predominantly localized to distinct puncta, which is consistent with the conclusion that micro ribonucleoprotein complexes aggregate in vivo. However, *dicer-1* puncta were scattered throughout postsynaptic muscle cells, and not obviously associated with any particular organelle, the perinuclear region, or postsynaptic densities, as previously described for mouse brain (Lugli et al., 2005).

Interestingly, *MiR-284* regulated GluR protein abundance in proportion to the number of predicted binding sites in each target transcript: *GluRIIB* had two predicted *MiR-284* binding sites, and was most strongly affected by loss of *MiR-284*; *GluRIIA*,

a deletion [*Df(3R)kar-Sz12*] that removes *MiR-284* show abundant mislocalized GluRIIA and GluRIIB in body wall muscles. (C) Quantification from images like that shown in B. GluRIIB protein is dramatically increased both in synapses and in nonsynaptic (intracellular) areas, whereas GluRIIA is increased only nonsynaptically ($n = 10–12$). ***, $P < 0.0001$. (D) GluRIIC is not changed in *MiR-284* deletion mutants [*Df(3R)kar-Sz12*; $n = 5$]. Error bars represent SEM. n.s., not significant.

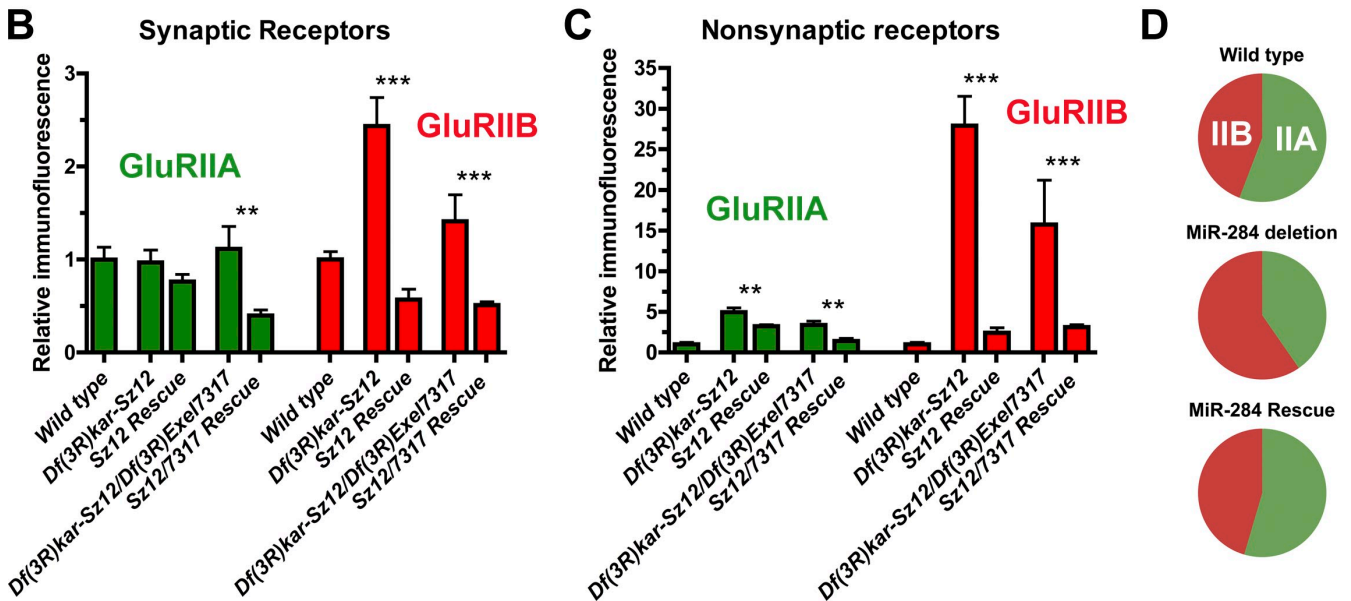
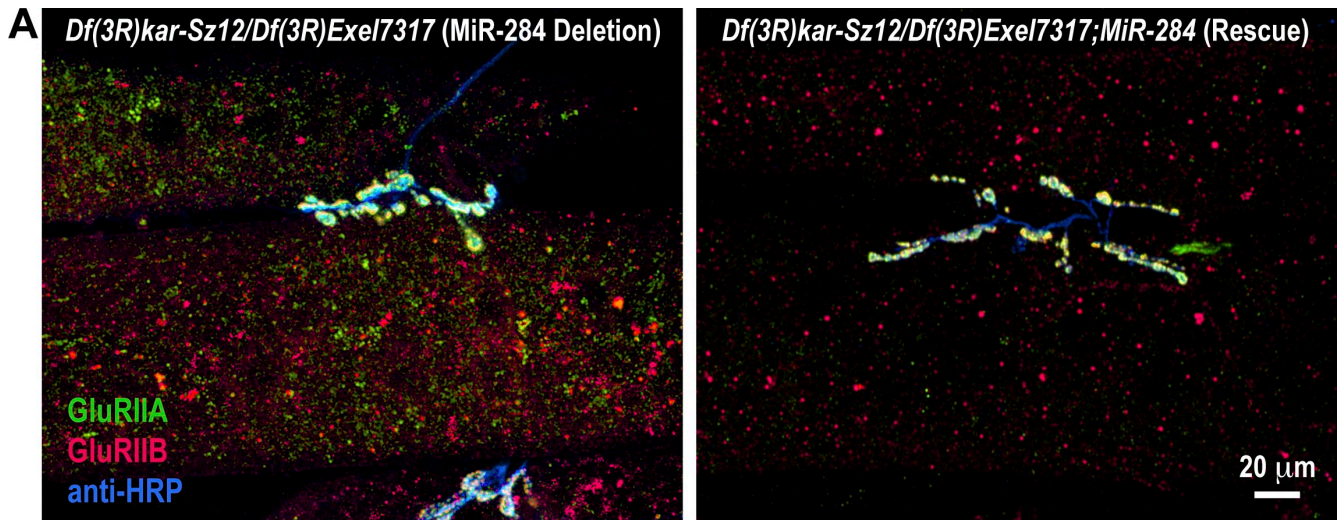


Figure 9. **A** *Mir-284* transgene rescues GluR phenotypes caused by deletion of the native *Mir-284* gene. (A) Larvae hemizygous for each of two different *Mir-284* deletions [*Df(3R)kar-Sz12/Df(3R)exel7317*] show abundant mislocalized GluRIIA and GluRIIB in body wall muscles (left), and this phenotype is largely rescued with a single copy of a *Mir-284* transgene (right). (B and C) Quantification of synaptic (B) and nonsynaptic (C) GluRIIA and GluRIIB immunoreactivity (green and red, respectively) for homozygous *Df(3R)kar-Sz12* mutants, mutants of the genotype *Df(3R)kar-Sz12/Df(3R)exel7317*, and each of these two mutants expressing a *Mir-284* transgene. Error bars represent SEM. n.s., not significant. ***, $P < 0.0001$. (D) Pie charts showing relative amounts of GluRIIA and GluRIIB immunoreactivity in control NMJs, in NMJs after deletion of *Mir-284*, and in *Mir-284* deletion mutants rescued with a *Mir-284* transgene.

with one predicted binding site, was less affected; and *GluRIIC*, with no predicted binding sites, was not affected at all. This suggests that microRNA-mediated regulation of any particular transcript may depend on the number and type of individual microRNA-binding sites, where more potential binding sites lead to stronger repression. Also, interestingly, none of the predicted *Mir-284* binding sites in either *GluRIIA* or *GluRIIB* were in UTRs.

However, as noted, we were unable to obtain consistent a priori bioinformatic predictions regarding the number and type of microRNA-binding sites in *Drosophila* GluR transcripts. Even the experimentally supported prediction that *Mir-284* binds to GluR mRNAs was not generally replicable using most bioinformatics tools, including, importantly, later versions of

the program (MicroInspector) that made the original prediction. These sorts of bioinformatics inconsistencies have been commented upon by others (Bartel, 2009), and demonstrate that the molecular mechanisms by which microRNAs interact with their targets in vivo are still imperfectly understood or not yet consistently implemented in publicly accessible computational form. However, it is important to note that we were eventually able to successfully predict *Mir-284* regulation of *GluRIIA* and *GluRIIB* using a combination of bioinformatic “tuning” and preliminary biological data. We therefore think that computational tools for prediction of microRNA–target interactions remain an important goal, and deserve high priority given the obvious usefulness that accurate algorithms will have.

Materials and methods

UAS-dicer-1 transgene construction

The UAS-dcr1-IR (*UAS-dicer.RNAi*) transgene was created using previously described methods and reagents (Lee and Carthew, 2003). In brief, a 513-bp *dicer-1*-specific PCR product was amplified from genomic DNA using primers 5' XbaDcr1 (5'-TTAGTCTAGAACAACTTGACGACTC-CAATGATAGC-3') and 3' XbaDcr1 (5'-TTAGTCTAGAAAATGAGGTAATC-TAGAACAGCATCGC-3'). This PCR product was digested with Xba and ligated "tail-to-tail" into the AvrII site of the pWIZ vector (Lee and Carthew, 2003). This construct was then used to transform *yw[67c23]* flies according to standard methods (Spradling and Rubin, 1982). Two independent transgene insertion lines were obtained and mapped to chromosomes 2 and 3. We expressed *UAS-dcr1.RNAi* transgenes using two different Gal4 drivers: *TubGal4*, which drives in all tissues (Lee and Luo, 1999), and *24BGal4*, which drives exclusively in mesoderm (muscle; Brand and Perrimon, 1993).

UAS-MiR-284 transgene construction

The "rescue" transgene containing the *MiR-284* genomic region was created using the Gateway cloning system (Invitrogen). To clone the *MiR-284* genomic region, we PCR-amplified the 21-bp *MiR-284* gene (5'-TGAAGTCAGCAACT-GATCCAGCAATTG-3') plus an additional 1 kb in the upstream direction, and 300 bp in the downstream direction. Primers were designed with *attB* sites added according to the Gateway cloning protocol. The primers were: *MiR284 L3* (5'-AGAATCCCTGGGTAATCAGCAGAATG-3') and *MiR284 R3* (5'-ATTAGATCTTCAACGACAATCGCATGAAT-3'). The pUAST Gateway destination vector was designed by B. Ackley (University of Kansas, Lawrence, KS) using the Gateway Vector Conversion System (Invitrogen). The pUAST: *MiR-284* transgene was then sequenced and transformed using standard methods (Spradling and Rubin, 1982).

All rescue animals were individually genotyped using PCR to confirm that the native *MiR-284* gene was deleted and that they also carried the *MiR-284* transgene, as follows. First, we confirmed that the native *MiR-284* gene was deleted using primers 5'-CCAAAATCGCAGAGGACAT-3' and 5'-GTCGTGGATCTGACCCTTG-3'. These primers produce a 762-bp band when the wild-type genomic region is present; a negative PCR result indicated the larva was homozygous for the *MiR-284* deletion. *Actin 5C* was used as a positive control for the PCR reaction, using primers 5'-GCAC-CACACCTTCTACAATGAGC-3' and 5'-TACAGCGAGAGCAGCCCTG-GATG-3', which amplify a 171-bp region of the *actin 5C* gene.

Real-time RT-PCR and quantification of GluR mRNA abundance

For real-time RT-PCR, RNA isolation, reverse transcription, and PCR was performed as described previously (Featherstone et al., 2005; Liebl et al., 2005; Liebl et al., 2006), with slight modifications for more precise quantification. In brief, *Drosophila* total RNA was isolated from several animals of each genotype using standard TRIZOL extraction (Roberts, 1998), and then reversed transcribed using poly dT primers. Real-time PCR was then performed on mRNAs of interest (*GluRIIA*, *GluRIIB*, and the control/standard *actin 5c*) using a thermocycler (Opticon 2; MJ Research) with SYBR green for amplicon detection and quantitation. Quantification of starting mRNA was computed according to Horz et al. (2004). In brief, the cycle threshold ($C(t)$) values for the target (*GluRIIA* or *GluRIIB*) and an *actin 5C* control were determined for each sample, and the target was normalized to the control using the following calculation: $\Delta C(t)_{\text{sample}} = C(t)_{\text{target}} - C(t)_{\text{actin 5C}}$. Normalized sample $C(t)$ values were then referenced to a wild-type control sample (the "calibrator") to determine the relative amount of target mRNA in the test sample. The formula used for determining relative target levels was: $\Delta\Delta C(t)_{\text{sample}} = \Delta C(t)_{\text{sample}} - \Delta C(t)_{\text{calibrator}}$. The amount of target for each sample is reported as a ratio relative to the calibrator using: $2^{-\Delta\Delta C(t)}$. Essentially, *actin 5C* serves as a control for RNA isolation and amplification in each sample, and the wild type provides a standard quantity of target transcript to which all samples are referenced. Other aspects of the calculation correct for the fact that PCR product abundance is logarithmically (rather than linearly) related to the starting template.

FISH

RNA probes were synthesized in vitro from full-length target cDNAs, using standard methods appropriate to the cDNA vector (e.g., SP6 RNA polymerase for vectors containing an SP6 promoter). cDNAs for *GluRIIA* and *GluRIIB* were gifts from S. Sigris (Freie Universität Berlin, Berlin, Germany); *GluRIIC* cDNA was obtained from the *Drosophila* Genomics Resource Center. After synthesis, probes were shortened using alkaline hydrolysis for better penetration of tissues (Cox et al., 1984), and precipitated using

standard methods. In most cases, the probe was labeled with digoxigenin-UTP (DIG-UTP; Roche) during transcription and then eventually visualized using anti-DIG antibodies. In some cases, the synthesis reaction included an amine-modified UTP that could be subsequently directly labeled with a fluorophore ("FISH tag" kit; Invitrogen). In situ hybridization was then performed using standard methods similar to those described previously (Braissant and Wahli, 1998; Sigris et al., 2000; Tomancak et al., 2002). In brief, manually filleted third instar larvae were fixed for 1 h in 4% paraformaldehyde in phosphate-buffered saline, and then permeabilized using TritonX-100. After fixation, larvae were incubated with probes at 55°C overnight, then stained with anti-HRP antibodies to visualize NMs, and with either anti-DIG antibodies or fluorophores with affinity to amine-modified UTP for visualization of mRNA using confocal fluorescent microscopy.

Immunocytochemistry and confocal microscopy

For immunocytochemistry and confocal microscopy, animals were manually dissected and fixed in Bouin's fixative, as described previously (Chen and Featherstone, 2005; Chen et al., 2005). *Drosophila dicer-1* mouse polyclonal antibody (A1031a; used at 1:1,000) was generated against the *dicer-1*-specific peptide TRHLYEDPRQHSPGALTLDR by the CIM antibody core at Arizona State University, but is no longer available from this source due to loss of funding. Mouse monoclonal anti-GluRIIA, from a cell line made by C. Schuster (University of Heidelberg, Heidelberg, Germany) and available from University of Iowa's Developmental Studies Hybridoma Bank, was used at 1:100–1:200 (Featherstone et al., 2002). Rabbit polyclonal anti-GluRIIB and rabbit polyclonal anti-GluRIIC, first described in Marrus et al. (2004) and subsequently replicated in our own laboratory (Liebl et al., 2005), were used at 1:2,000. Fluorescently conjugated anti-HRP was used at 1:100–1:200. Immunoreactivity was visualized using FITC, TRITC, or CY5-conjugated goat anti-mouse/rabbit secondary antibodies (Jackson ImmunoResearch Laboratories) at 1:400. For plasma membrane staining using the fixable membrane dye FM1-43FX (Invitrogen), dissected larval preparations were exposed to 5 µg/ml FM1-43FX in ice-cold phosphate-buffered saline for 1 min, then fixed immediately in Bouin's fixative. For imaging, preparations were mounted on slides in Vectashield mounting medium (Vector Laboratories). All images of NMs are from ventral longitudinal muscles 6 and 7 in abdominal segments 3 and 4. Control and experimental preparations were always stained and imaged in parallel.

Images were captured using a laser scanning confocal system (Fluoview FV500; Olympus) running Fluoview software 4.3 with a 40x/1.3 NA UPlan-Fluar or a 60x/1.4 NA Plan-Apochromat objective lens (Olympus). All imaging was performed at room temperature (20–23°C). Quantification of staining intensity was performed as described previously (Featherstone et al., 2001). In brief, fluorescence intensity of relevant structures from unaltered, unsaturated confocal maximum intensity projections was measured by manually selecting the region of interest in ImageJ and measuring the mean pixel intensity of that region. To control for differences in individual preparation immunoreactivity, excitation, fluorescence attenuation, and detection, we then subtracted the mean pixel intensity of a similarly sized region of unstained "background" in the same fluorescence wavelength channel in the same image. 3D isosurface reconstructions were performed using Amira 3.1 (Mercury Computer Systems). Photoshop CS2 was then used to crop images and adjust contrast for printing.

Microscopic puncta (*dicer-1* immunoreactivity or *GluR* mRNA aggregates detected by FISH; Figs. 1 C and 2 B) were counted manually or using Particle Counting macros in ImageJ 1.42 (<http://rsb.info.nih.gov/ij/>). Both methods yield similar results. Spots that were 1–2 pixels in total size were in both cases assumed to be noise, and therefore not counted.

Electrophysiology

All electrophysiological recordings were obtained from larval ventral longitudinal muscle 6 (A3–4) using a two-electrode voltage clamp (–60 mV) as described previously (Featherstone et al., 2000, 2005; Liebl et al., 2005). Note that this is the same NM that was analyzed for all other experiments in this study. All dissections and electrophysiology were performed under standard *Drosophila* saline (135 mM NaCl, 5 mM KCl, 4 mM MgCl₂, 1.8 mM CaCl₂, 5 mM TES [Tris, EDTA, and NaCl], and 72 mM sucrose).

Statistics

Statistical significance was determined using unpaired Student's *t* tests (for normally distributed data) or nonparametric Mann-Whitney tests (when post-hoc *F*-tests determined that variances were significantly different). sEJC amplitude distributions were compared using Kolmogorov-Smirnov tests. In all figures, asterisks indicate statistical significance (*, $P < 0.01$; **, $P < 0.001$; ***, $P < 0.0001$), "n.s." indicates a lack of statistical significance (i.e., "not significant"), and error bars represent SEM.

Bioinformatics

Online supplemental material includes three Microsoft Excel files converted from comma-delimited .csv data files, which represent output from MicroInspector (version 1.0; Rusinov et al., 2005). Each of these files was generated using MicroInspector 1.0 default/recommended parameters (Hybridization temperature 25°C, -26 kcal/mole free energy cutoff). Rows are sorted by free energy, where the most likely interactions are listed first. As described in the text, our experimental results support only the most likely two interactions for GluRIIA and GluRIIB, and none of the interactions for GluRIIC. Note that algorithms in subsequent versions of MicroInspector have been modified, and results from the current online version may not be identical to those described here.

Online supplemental material

Table S1 is the MicroInspector output after the Flybase 5.2 GluRIIA transcript sequence was used as input. Table S2 is the MicroInspector output after the Flybase 5.2 GluRIIB transcript sequence was used as input. Table S3 is the MicroInspector output after the Flybase 5.2 GluRIIC transcript sequence was used as input. Online supplemental material is available at <http://www.jcb.org/cgi/content/full/jcb.200902062/DC1>.

The authors would like to thank Pei-San Ng for technical assistance, Dr. Richard Carthew for advice and suggestions early in this project, and Dr. Brian Ackley for making the pUAST Gateway cloning vector used to make the MiR-284 transgene. We also give special thanks to Dr. Vesselin Baev for assistance with MicroInspector. The University of Iowa Developmental Studies Hybridoma bank, Bloomington Stock Center, and the University of Illinois at Chicago's Research Resource Center provided essential reagents and services.

This work was funded by National Institutes of Health/National Institute of Neurological Disorders and Stroke grant R01NS045628 to D. Featherstone, and by the Russian Academy of Sciences Program on Cell Molecular Biology.

Submitted: Submitted: 12 February 2009

Accepted: Accepted: 13 April 2009

References

Baek, D., J. Villen, C. Shin, F.D. Camargo, S.P. Gygi, and D.P. Bartel. 2008. The impact of microRNAs on protein output. *Nature*. 455:64–71.

Bartel, D.P. 2009. MicroRNAs: target recognition and regulatory functions. *Cell*. 136:215–233.

Berezikov, E., E. Cuppen, and R.H. Plasterk. 2006. Approaches to microRNA discovery. *Nat. Genet.* 38:S2–S7.

Bernstein, E., A.A. Caudy, S.M. Hammond, and G.J. Hannon. 2001. Role for a bidentate ribonuclease in the initiation step of RNA interference. *Nature*. 409:363–366.

Bicker, S., and G. Schratt. 2008. microRNAs: tiny regulators of synapse function in development and disease. *J. Cell. Mol. Med.* 12:1466–1476.

Braissant, O., and W. Wahli. 1998. Differential expression of peroxisome proliferator-activated receptor- α , - β , and - γ during rat embryonic development. *Endocrinology*. 139:2748–2754.

Bramham, C.R. 2008. Local protein synthesis, actin dynamics, and LTP consolidation. *Curr. Opin. Neurobiol.* 18:524–531.

Brand, A.H., and N. Perrimon. 1993. Targeted gene expression as a means of altering cell fates and generating dominant phenotypes. *Development*. 118:401–415.

Brennecke, J., A. Stark, R.B. Russell, and S.M. Cohen. 2005. Principles of microRNA-target recognition. *PLoS Biol.* 3:e85.

Broadie, K., and M. Bate. 1993. Innervation directs receptor synthesis and localization in *Drosophila* embryo synaptogenesis. *Nature*. 361:350–353.

Cao, X., G. Yeo, A.R. Muotri, T. Kuwabara, and F.H. Gage. 2006. Noncoding RNAs in the mammalian central nervous system. *Annu. Rev. Neurosci.* 29:77–103.

Chen, K., and D.E. Featherstone. 2005. Discs-large (DLG) is clustered by presynaptic innervation and regulates postsynaptic glutamate receptor subunit composition in *Drosophila*. *BMC Biol.* 3:1.

Chen, K., C. Merino, S.J. Sigrist, and D.E. Featherstone. 2005. The 4.1 protein coracle mediates subunit-selective anchoring of *Drosophila* glutamate receptors to the postsynaptic actin cytoskeleton. *J. Neurosci.* 25:6667–6675.

Cox, K.H., D.V. DeLeon, L.M. Angerer, and R.C. Angerer. 1984. Detection of mRNAs in sea urchin embryos by in situ hybridization using asymmetric RNA probes. *Dev. Biol.* 101:485–502.

DiAntonio, A., S.A. Petersen, M. Heckmann, and C.S. Goodman. 1999. Glutamate receptor expression regulates quantal size and quantal content at the *Drosophila* neuromuscular junction. *J. Neurosci.* 19:3023–3032.

Enright, A.J., B. John, U. Gaul, T. Tuschl, C. Sander, and D.S. Marks. 2003. MicroRNA targets in *Drosophila*. *Genome Biol.* 5:R1.

Featherstone, D.E., and K. Broadie. 2004. Physiological maturation of the neuromuscular system. In *Comprehensive Molecular Insect Science*. L. Gilbert, K. Iatrou, and S. Gill, editors. Pergamon Press, Amsterdam/Boston. 85–134.

Featherstone, D.E., E.M. Rushton, M. Hilderbrand-Chae, A.M. Phillips, F.R. Jackson, and K. Broadie. 2000. Presynaptic glutamic acid decarboxylase is required for induction of the postsynaptic receptor field at a glutamatergic synapse. *Neuron*. 27:71–84.

Featherstone, D.E., W.S. Davis, R.R. Dubreuil, and K. Broadie. 2001. *Drosophila* alpha- and beta-spectrin mutations disrupt presynaptic neurotransmitter release. *J. Neurosci.* 21:4215–4224.

Featherstone, D.E., E. Rushton, and K. Broadie. 2002. Developmental regulation of glutamate receptor field size by nonvesicular glutamate release. *Nat. Neurosci.* 5:141–146.

Featherstone, D.E., E. Rushton, J. Rohrbough, F. Liebl, J. Karr, Q. Sheng, C.K. Rodesch, and K. Broadie. 2005. An essential *Drosophila* glutamate receptor subunit that functions in both central neuropil and neuromuscular junction. *J. Neurosci.* 25:3199–3208.

Fiore, R., G. Siegel, and G. Schratt. 2008. MicroRNA function in neuronal development, plasticity and disease. *Biochim. Biophys. Acta.* 1779:471–478.

Giraldez, A.J., R.M. Cinalli, M.E. Glasner, A.J. Enright, J.M. Thomson, S. Baskerville, S.M. Hammond, D.P. Bartel, and A.F. Schier. 2005. MicroRNAs regulate brain morphogenesis in zebrafish. *Science*. 308:833–838.

Horz, H.-P., R. Kurtz, D. Batey, and B. Bohannan. 2004. Monitoring microbial populations using real-time qPCR on the MJ research Opticon 2 system. *MJ Research Application Note*. 3:1–4.

Hutvagner, G., J. McLachlan, A.E. Pasquinelli, E. Balint, T. Tuschl, and P.D. Zamore. 2001. A cellular function for the RNA-interference enzyme Dicer in the maturation of the let-7 small temporal RNA. *Science*. 293:834–838.

Job, C., and J. Eberwine. 2001. Localization and translation of mRNA in dendrites and axons. *Nat. Rev. Neurosci.* 2:889–898.

Keshishian, H., K. Broadie, A. Chiba, and M. Bate. 1996. The *Drosophila* neuromuscular junction: a model system for studying synaptic development and function. *Annu. Rev. Neurosci.* 19:545–575.

Krek, A., D. Grun, M.N. Poy, R. Wolf, L. Rosenberg, E.J. Epstein, P. MacMenamin, I. da Piedade, K.C. Gunsalus, M. Stoffel, and N. Rajewsky. 2005. Combinatorial microRNA target predictions. *Nat. Genet.* 37:495–500.

Lee, C.T., T. Risom, and W.M. Strauss. 2007. Evolutionary conservation of microRNA regulatory circuits: an examination of microRNA gene complexity and conserved microRNA-target interactions through metazoan phylogeny. *DNA Cell Biol.* 26:209–218.

Lee, J., A. Ueda, and C.F. Wu. 2008. Pre- and post-synaptic mechanisms of synaptic strength homeostasis revealed by slowpoke and shaker K(+) channel mutations in *Drosophila*. *Neuroscience*. 154:1283–1296.

Lee, T., and L. Luo. 1999. Mosaic analysis with a repressible cell marker for studies of gene function in neuronal morphogenesis. *Neuron*. 22:451–461.

Lee, Y.S., and R.W. Carthew. 2003. Making a better RNAi vector for *Drosophila*: use of intron spacers. *Methods*. 30:322–329.

Lee, Y.S., K. Nakahara, J.W. Pham, K. Kim, Z. He, E.J. Sontheimer, and R.W. Carthew. 2004. Distinct roles for *Drosophila* Dicer-1 and Dicer-2 in the siRNA/miRNA silencing pathways. *Cell*. 117:69–81.

Liebl, F.L., K. Chen, J. Karr, Q. Sheng, and D.E. Featherstone. 2005. Increased synaptic microtubules and altered synapse development in *Drosophila* sec8 mutants. *BMC Biol.* 3:27.

Liebl, F.L., K.M. Werner, Q. Sheng, J.E. Karr, B.D. McCabe, and D.E. Featherstone. 2006. Genome-wide P-element screen for *Drosophila* synaptogenesis mutants. *J. Neurobiol.* 66:332–347.

Lugli, G., J. Larson, M.E. Martone, Y. Jones, and N.R. Smalheiser. 2005. Dicer and eIF2c are enriched at postsynaptic densities in adult mouse brain and are modified by neuronal activity in a calpain-dependent manner. *J. Neurochem.* 94:896–905.

Lugli, G., V.I. Torvik, J. Larson, and N.R. Smalheiser. 2008. Expression of microRNAs and their precursors in synaptic fractions of adult mouse forebrain. *J. Neurochem.* 106:650–661.

Marrus, S.B., S.L. Portman, M.J. Allen, K.G. Moffat, and A. DiAntonio. 2004. Differential localization of glutamate receptor subunits at the *Drosophila* neuromuscular junction. *J. Neurosci.* 24:1406–1415.

Martin, K.C., and R.S. Zukin. 2006. RNA trafficking and local protein synthesis in dendrites: an overview. *J. Neurosci.* 26:7131–7134.

Miller, S., M. Yasuda, J.K. Coats, Y. Jones, M.E. Martone, and M. Mayford. 2002. Disruption of dendritic translation of CaMKII α impairs stabilization of synaptic plasticity and memory consolidation. *Neuron*. 36:507–519.

- Murchison, E.P., J.F. Partridge, O.H. Tam, S. Cheloufi, and G.J. Hannon. 2005. Characterization of Dicer-deficient murine embryonic stem cells. *Proc. Natl. Acad. Sci. USA.* 102:12135–12140.
- Nishikawa, K., and Y. Kidokoro. 1995. Junctional and extrajunctional glutamate receptor channels in *Drosophila* embryos and larvae. *J. Neurosci.* 15:7905–7915.
- Okamura, K., A. Ishizuka, H. Siomi, and M.C. Siomi. 2004. Distinct roles for Argonaute proteins in small RNA-directed RNA cleavage pathways. *Genes Dev.* 18:1655–1666.
- Pfeiffer, B.E., and K.M. Huber. 2006. Current advances in local protein synthesis and synaptic plasticity. *J. Neurosci.* 26:7147–7150.
- Qin, G., T. Schwarz, R.J. Kittel, A. Schmid, T.M. Rasse, D. Kappei, E. Ponimaskin, M. Heckmann, and S.J. Sigrist. 2005. Four different subunits are essential for expressing the synaptic glutamate receptor at neuromuscular junctions of *Drosophila*. *J. Neurosci.* 25:3209–3218.
- Rajewsky, N. 2006. microRNA target predictions in animals. *Nat. Genet.* 38:S8–S13.
- Roberts, D.B. 1998. *Drosophila: A Practical Approach*, 2nd Edition. Oxford University Press, Oxford. 389 pp.
- Ruiz-Canada, C., and V. Budnik. 2006. Introduction on the use of the *Drosophila* embryonic/larval neuromuscular junction as a model system to study synapse development and function, and a brief summary of pathfinding and target recognition. *Int. Rev. Neurobiol.* 75:1–31.
- Rusinov, V., V. Baev, I.N. Minkov, and M. Tabler. 2005. MicroInspector: a web tool for detection of miRNA binding sites in an RNA sequence. *Nucleic Acids Res.* 33:W696–W700.
- Schmid, A., S. Hallermann, R.J. Kittel, O. Khorramshahi, A.M. Frolich, C. Quentin, T.M. Rasse, S. Mertel, M. Heckmann, and S.J. Sigrist. 2008. Activity-dependent site-specific changes of glutamate receptor composition in vivo. *Nat. Neurosci.* 11:659–666.
- Schuman, E.M., J.L. Dynes, and O. Steward. 2006. Synaptic regulation of translation of dendritic mRNAs. *J. Neurosci.* 26:7143–7146.
- Selbach, M., B. Schwanhausser, N. Thierfelder, Z. Fang, R. Khanin, and N. Rajewsky. 2008. Widespread changes in protein synthesis induced by microRNAs. *Nature.* 455:58–63.
- Sethupathy, P., B. Corda, and A.G. Hatzigeorgiou. 2006. TarBase: A comprehensive database of experimentally supported animal microRNA targets. *RNA.* 12:192–197.
- Sigrist, S.J., P.R. Thiel, D.F. Reiff, P.E. Lachance, P. Lasko, and C.M. Schuster. 2000. Postsynaptic translation affects the efficacy and morphology of neuromuscular junctions. *Nature.* 405:1062–1065.
- Simon, D.J., J.M. Madison, A.L. Conery, K.L. Thompson-Peer, M. Soskis, G.B. Ruvkun, J.M. Kaplan, and J.K. Kim. 2008. The microRNA miR-1 regulates a MEF-2-dependent retrograde signal at neuromuscular junctions. *Cell.* 133:903–915.
- Spradling, A.C., and G.M. Rubin. 1982. Transposition of cloned P elements into *Drosophila* germ line chromosomes. *Science.* 218:341–347.
- Stark, A., J. Brennecke, R.B. Russell, and S.M. Cohen. 2003. Identification of *Drosophila* MicroRNA targets. *PLoS Biol.* 1:E60.
- Sutton, M.A., and E.M. Schuman. 2005. Local translational control in dendrites and its role in long-term synaptic plasticity. *J. Neurobiol.* 64:116–131.
- Sutton, M.A., N.R. Wall, G.N. Aakalu, and E.M. Schuman. 2004. Regulation of dendritic protein synthesis by miniature synaptic events. *Science.* 304:1979–1983.
- Tomancak, P., A. Beaton, R. Weiszmam, E. Kwan, S. Shu, S.E. Lewis, S. Richards, M. Ashburner, V. Hartenstein, S.E. Celniker, and G.M. Rubin. 2002. Systematic determination of patterns of gene expression during *Drosophila* embryogenesis. *Genome Biol.* 3:RESEARCH0088.
- Watanabe, Y., M. Tomita, and A. Kanai. 2007. Computational methods for microRNA target prediction. *Methods Enzymol.* 427:65–86.